Generalized Fokker-Planck Approach to the Coupling Model and Comparison with Computer Simulations

K. L. Ngai*

Naval Research Laboratory, Washington, D.C. 20375-5000

S. L. Peng

School of Physics, Georgia Institute of Technology, Atlanta, Georgia 30332

Jeffrey Skolnick

Department of Molecular Biology, The Scripps Research Institute, 10666 North Torrey Pines Road, La Jolla, California 92037

Received August 7, 1991; Revised Manuscript Received January 6, 1992

ABSTRACT: The coupling model is reformulated using a Fokker-Planck approach to generalize the Rouse model to include time-dependent rate slowing down by entanglement coupling. The results compare favorably with data of several computer simulations. In particular, we point out the results of the normal-mode analysis of the molecular dynamics simulations of Kremer and Grest are in good agreement with the coupling model but at variance with the reptation model.

I. Introduction

A scheme for incorporating the effects of entanglements on the dynamics of Rouse modes has been proposed some while ago by one of us[1-6] and collaborators. Since then, predictions of the model have been applied to explain the viscoelasticity and self-diffusion in melts as well as related problems in solutions. In the past, the results were based on the master equation approach. This coupling scheme modifies the pth Rouse mode by slowing down its relaxation rate τ_p^{-1} by the reduction factor $(\omega_c t)^{-n_p}$. Here ω_c is the reciprocal of the time t_c to cross over from the short-time pure Rouse[7,8] dynamics to the slowed-down dynamics caused by many-chain "topological" interactions or entanglement couplings. The exponent n_p, called the coupling parameter, is a measure of the degree of rate slowing down of the pth mode. For flexible polymer melts, there is a length scale N_e such that, if the chain length N is shorter than N_e, all Rouse modes (including the diffusion $p = 0$ mode and the most cooperative, $p = 1$, intramolecular mode) are unretarded. That is, in the coupling scheme

$$n_p = 0, \quad \text{for all } p\text{'s} \tag{1}$$

if $N < N_e$. This corresponds to the empirical fact that, for real polymer melts satisfying the condition $N < N_e$, their viscoelastic properties are well described by the Rouse model (suitably modified for undiluted polymers[8]). In the entangled regime when $N > N_e$, the coupling model requires that some n_p's become nonzero. This property of the coupling parameters means that the coupling model possesses an intermediate characteristic length scale which is the entanglement distance N_e. Above N_e, the viscoelastic and self-diffusion properties increasingly deviate from Rouse behavior. After $N > N_c$, where N_c is typically a few times larger than N_e, the non-Rousean behavior settles down into a well-defined pattern; e.g., the terminal relaxation time, τ_η*, scales[9] like $N^{3.4}$.

In the transition to the entangled regime, i.e., as N increases beyond N_e, some n_p's will start to assume nonzero values and increase with N. Intuitively, we would expect the intramolecularly most cooperative $p = 1$ mode with the longest wavelength to be the first to become nonzero. For $N > N_e$ we have previously[1] proposed that

$$n_p > n_{p'}, \quad \text{for } 1 \le p < p' \tag{2}$$

Beyond N_c, after which the polymer is fully entangled, we have found that n_1 attains a maximum constant value of about 0.41. This conclusion follows from a comparison between one of several predictions of the coupling model with the time and frequency dependence of the terminal[1] relaxation of near monodisperse melts.

In the fully entangled regime of $N > N_c$, we consider, for convenience, cases where the chain length N is an integral multiple of N_e; i.e.

$$N = p_e N_e \tag{3}$$

where p_e is an integer. The p_eth Rouse mode of the N chain here resembles the first Rouse mode of the shorter chain with length N_e in the sense that the former can be considered as the latter repeated p_e times. Hence, the coupling parameter, $n_{p_e}(N)$, of the p_eth Rouse mode of the N chain is the same as $n_1(N_e)$ of the first Rouse mode of the N_e chain. From eq 1, it follows that

$$n_p(N) = 0, \quad \text{for } p \ge p_e \tag{4}$$

The coupling parameters for the lower modes with $p = p_e - 1, p_e - 2, \ldots, 1$ can be nonzero. These modes whose wavelengths are longer than the entanglement length scale, N_e, are susceptible to rate slowing down by entanglement coupling which makes n_p nonzero for $p < p_e$. We expect also the inequalities

$$0 < n_{p_e-1}(N) < n_{p_e-2}(N) < \ldots < n_1(N) \le 0.41 \tag{5}$$

because when the Rouse mode number p decreases, the motion involved becomes more cooperative along the chain and more susceptible to rate slowing down by intermolecular (entanglements) couplings with other chains. In the fully entangled regime, the coupling parameter n_1 remains constant at the value of about 0.41.[1,19,21] On the basis of this value of n_1, an additional prediction (see eq 19 in section II or eq 37 in section III of this paper) of the coupling model has enabled us to derive[1-4] the $\eta \sim N^{3.4}$ law for the viscosity[8] and other properties. Although the coupling model has not been established as yet on rigorous

0024-9297/92/2225-2184$03.00/0

theoretical foundations, there are strong indications that its results are the natural consequences of some general physical principles[9] governing the relaxation of correlated systems with nonintegrable (i.e., nonharmonic) many-body interactions.

In this work, we shall reformulate the coupling scheme in the framework of the generalized Fokker-Planck[10] equation. The advantage of this formulation is that various autocorrelation functions of experimental interest can be conveniently obtained. The center-of-mass mean-square displacement correlation function has been considered in a recent paper[11] where good agreement between the predictions of the coupling model and Monte Carlo[12,13] as well as molecular-dynamics[14] simulations has been pointed out. Here, other correlation functions are obtained and considered in our continued comparisons with computer simulations.

II. Coupling Scheme in the Fokker-Planck Equation Approach

The Rouse theory has been formulated based on the Fokker-Planck equation. For the case of steady-state flow without external field, the diffusion equation of the Fokker-Planck type can be written as[15]

$$\frac{\partial P}{\partial t} = k_B T \frac{\nu_0}{\zeta_0} \frac{\partial^2 P}{\partial \xi_0^2} + \frac{K}{\zeta_0} \sum_{p=1}^{N-1} \left\{ \lambda_p \frac{\partial}{\partial \xi_p}(\xi_p P) + k_B T \frac{\nu_p}{\xi_0} \frac{\partial^2 P}{\partial \xi_p^2} \right\} \quad (6)$$

A review of the mathematical formalism has been given by Skolnick and Yaris (SY).[15] The quantities appearing in eq 6 have been defined by SY, and we shall follow the notation presented there, except that N replaces n used by SY to denote the number of beads in a polymer chain. The constant diffusion coefficient and drift for each mode are respectively

$$\beta_p = \frac{K}{\zeta_0}\lambda_p \equiv \lambda_p / 2t_0 \quad (7)$$

and

$$\gamma_p = \frac{k_B T}{\zeta_0}\nu_p \quad (8)$$

where

$$K = 3k_B T / b_0^2 \quad (9)$$

and

$$t_0 = \zeta_0 b_0^2 / 6k_B T \quad (10)$$

The relation between β_p and γ_p is

$$\gamma_p = \langle \xi_p^2 \rangle \beta_p \quad (11)$$

Equations 6-10 constitute a basic description of the Rouse-like chain. The coupling model (see section I) reduces to the Rouse theory in the regime $N \leq N_e$ where $n_p = 0$ for all p's.

To obtain a more general Fokker-Planck equation that can also describe the case of $N > N_e$ where entanglement couplings are significant, we shall employ the coupling scheme. The coupling model proposes that at short times, $t < \omega_c^{-1}$, the chains are unretarded by the entanglement coupling; they relax according to the Rouse model. Beyond ω_c^{-1}, Rouse modes with $p < p_e$ have their relaxation rate, τ_p^{-1}, slowed down by a time-dependent factor $(\omega_c t)^{-n_p}$. From eqs 7 and 10, it is clear that the coefficient β_p in the Fokker-Planck equation (eq 6) is proportional to the Rouse rate τ_p^{-1}. Hence, following the scheme of the coupling model, we modify it accordingly as

$$\beta_p(t) = \beta_p(\omega_c t)^{-n_p} \quad \omega_c t > 1 \quad (12)$$

which reduces to the Rouse constant β_p when $n_p = 0$. It is natural also to generalize eq 11 for γ_p as

$$\gamma_p(t) = \langle \xi_p^2 \rangle \beta_p(t) \quad (13)$$

From these we obtain a generalized Fokker-Planck equation for the coupling model

$$\partial_t P = \sum_{p=0}^{N-1} (\beta_p(\tau)\, \partial_{\xi_p}(\xi_p P) + \gamma_p(t) \partial_{\xi_p \xi_p} P) \quad (14)$$

where $P(\xi_0, \xi_1, ..., \xi_{N-1})$ is the probability of finding $\xi \equiv (\xi_0, ..., \xi_{N-1})$ at time t. Linearity enables eigenmode expansion to find the solution. The normal modes, ξ_p, are independent of each other, and P has the product form

$$P = P_0 P_1 ... P_{N-1} \quad (15)$$

$$P_p = P_p(\xi_p, t) \quad (16)$$

As a result, each mode is governed by its own equation

$$\partial_t P_p = \beta_p(t)\, \partial_{\xi_p}(\xi_p P_p) + \gamma_p(t)\, \partial_{\xi_p}{}^2 P_p \quad (17)$$

with solution (see Appendix)

$$P_p(\xi_p(t), \xi_p(0)) = [2\pi \langle \xi_p^2 \rangle [1 - \exp[-2(t/\tau_p^*)^{1-n_p}]]^{-3/2} \times \exp[-[\xi_p(t) - \xi_p(0) \exp[-(t/\tau_p^*)^{1-n_p}]]]^2 / \{2\langle \xi_p^2 \rangle \times [1 - \exp(-(t/\tau_p^*)^{1-n_p})]\} \quad (18)$$

Here τ_p^* is related to the Rouse relaxation time τ_p by the important equation

$$\tau_p^* = \{(1 - n_p)\omega_c^{n_p} \tau_p\}^{1/(1-n_p)} \quad (19)$$

The equilibrium state is defined by

$$dP_{eq}/dt = 0 \quad (20)$$

The above condition is equivalent to

$$P_{eq} = \lim P(\xi_0, ..., \xi_{N-1}, t) = \prod_{p=0}^{N-1} \{(2\pi \langle \xi_p^2 \rangle)^{1/2} \times \exp\{-|\xi_k|^2 / 2\langle \xi_k^2 \rangle\} \quad (21)$$

Following the same method as outlined by SY, we can calculate all autocorrelation functions of interest. The $p = 0$ mode and the mean-squared center-of-mass displacement correlation function $g_{cm}(t) = \langle |R_{cm}(t) - R_{cm}(0)|^2 \rangle / b_0^2$ from the coupling model has been discussed by Ngai and Skolnick.[11] The results are in good agreement with three major computer simulations[12-14] and will not be considered any further here. Here we confine our attention to various single-bead mean-square displacement correlation functions and the end-to-end vector autocorrelation function. For the former, we are mainly interested in the time regime of $t \ll \tau_0^*$, where τ_0^* is the very long relaxation time of the slowed-down $p = 0$ mode given by eq 19 for $p = 0$ and discussed in ref 11. Hence, we can neglect the contribution of the mean-square displacement of the center of mass to the various single-bead autocorrelation functions. In fact, this contribution will be dropped entirely throughout the remainder of this work. Various autocorrelation functions can be obtained by using the property of Gaussian

distribution. For any $p \neq 0$ mode

$$\langle[\xi_p(t) - \xi_p(0)][\xi_{p'}(t) - \xi_{p'}(0)]\rangle = 6\delta_{pp'}\langle\xi_p^2\rangle \times [1 - \exp[-(t/\tau_p^*)^{1-n_p}]] \quad (22)$$

The time-dependent normalized autocorrelation function of the center of resistance[15] is given by

$$g_{sr}(t) = \langle S_r(t)\, S_r(0)\rangle/\langle S_r^2\rangle = \sum_{p=1}^{N-1}\mu_p^{-1} \times \exp[-(t/\tau_p^*)^{1-n_p}]/\sum_{p=1}^{N-1}\mu_p^{-1} \quad (23)$$

The ith bead mean-square displacement function has the expression

$$g_i(t) = b_0^{-2}\langle|\mathbf{R}_i(t) - \mathbf{R}_i(0)|^2\rangle = 2\sum_{p=1}^{N-1}Q_{ip}^2\mu_p^{-1} \times [1 - \exp[-(t/\tau_p^*)^{1-n_p}]] \quad (24)$$

The quantity μ_p is related to $\langle\xi_p^2\rangle$, the mean-square value of the pth normal mode by

$$\langle\xi_p^2\rangle = \mu_p^{-1}b_0^2/3 \quad (25)$$

Q_{ip} are the Rouse eigenfunctions given by

$$Q_{ip} = \left(\frac{2}{N}\right)^{1/2}\cos\left[p\frac{\pi}{2N}(2i+1)\right], \quad 1 \le p \le N-1 \quad (26a)$$

and

$$\mu_p = 4\sin^2(p\pi/2N) \quad (26b)$$

Various average mean-square displacements per bead can be defined including $g_1(t)$ when the average is performed over the entire chain

$$g_1(t) = \frac{1}{N}\sum_{i=0}^{N-1}g_i(t) = \frac{2}{N}\sum_{p=1}^{N-1}\mu_p^{-1}[1 - \exp[-(t/\tau_p^*)^{1-n_p}]] \quad (27)$$

and $g_1^{\text{inner}}(t)$ if the average is over only the innermost, say, five monomers, then

$$g_1^{\text{inner}}(t) = \frac{1}{5}\sum_{i=(N-1)/2-2}^{(N-1)/2+2}g_i(t) \quad (28)$$

The autocorrelation function of the end-to-end vector

$$\langle\mathbf{R}(t)\cdot\mathbf{R}(0)\rangle = \sum_{p=1}^{N-1}(Q_{0p} - Q_{N-1,p})^2\mu_p^{-1}\exp[-(t/\tau_p^*)^{1-n_p}] \quad (29)$$

can be obtained also along the same lines.

III. Comparison with Computer Simulations

By now, several computer simulations of the dynamics of entangled linear polymer melts have been published.[12-14] Although results of computer simulations are limited by available computer time, they have given considerable insight into the dynamics, particularly in the crossover behavior from the unentangled to the entangled regime. In an earlier paper[11] we have pointed out that on the center-of-mass mean-square displacement, $g_{cm}(t)$, the results of three major simulations are in remarkable agreement with each other. Moreover, the common features of these simulations are as predicted by the coupling model. The coupling parameter n_0 (previously denoted by n_D[2,4,11]) for the $p = 0$ Rouse mode of diffusion has been previously determined using self-diffusion experimental data[2] for fully entangled melts to be 0.32 ± 0.01. The coupling model then would predict the dependence[11]

$$g_{cm}(t) \sim t^{1-n_0} = t^{0.68} \quad (30)$$

in the intermediate time regime, which is in good agreement with all computer simulations for the longest chains studied.[12-14] In the crossover from the unentangled to the entangled regime, n_0 increases monotonically with N from zero toward[11] the maximum value of 0.32 ± 0.01. The dependence of n_0 on N determined from the $g_{cm}(t)$ data allowed us to predict the N dependence of the diffusion constant via a relation similar to eq 19 of the coupling model.[11] Good agreement with computer simulations have also been achieved. We now turn our attention here to other aspects of the chain dynamics obtained by computer simulations.

A. Normal-Mode (Rouse) Analysis. A molecular-dynamics simulation by Kremer and Grest (KG)[14] has analyzed their chain dynamics data in terms of the Rouse normal modes designated as $\mathbf{X}_p(t)$ by KG which is $\xi_p(t)$ in our notation. They have shown that the Rouse modes are eigenmodes of the chains from their analysis of the static structure of the chains. KG obtained the relaxation functions

$$\phi_p(t) = \langle\mathbf{X}_p(t)\cdot\mathbf{X}_p(0)\rangle/\langle\mathbf{X}_p(0)\cdot\mathbf{X}_p(0)\rangle \quad (31)$$

of the modes and analyzed their results in detail.

For short chains with $N \le 50$, $\phi_p(t)$ follows a linear exponential decay $\exp[-(t/\tau_p)]$ for all $p \ge 1$. At fixed N, τ_p scales like $1/p^2$. In a semilog plot of $\ln\phi_p(t)$ against the reduced time, $tp^2/\tau N^2$, relaxations of the different modes collapse onto a single curve which is nearly a straight line (see Figure 14a,b of ref 14). The time τ is a standard unit of time for a Lennard-Jones fluid defined by KG. The exact conformation of $\phi_p(t)$ to Rouse scaling and time dependence verifies the empirically known Rouse behavior of all modes for short chains with $N \le N_e$. An estimate of 35 has been given for the entanglement length N_e by KG. Note $N = 50$ is less than $2N_e$, and Rouse behavior for $N = 50$ is not unexpected from our discussion in section I.

The situation is different for longer chains having $N > 2N_e$. The $N = 100$ data (see Figures 13c and 14c of ref 14) show deviations from the Rouse behavior in two ways. First, $\phi_p(t)$ for the lower (smaller p) modes is no longer a linear exponential function, $\exp[-(t/\tau_p)]$, where τ_p is the Rouse time. In a semilog plot of $\phi_p(t)$ versus t/τ, the departure manifests itself as a curve rather than a straight line, and the curvature increases with decreasing p. Second, $\phi_p(t)$ of the lower modes cannot be reduced to collapse onto a single curve by scaling the time by the Rouse factor p^2/N^2. (N.B., we use the word "curve" instead of straight line because $\phi_p(t)$ for $p < 4$ are no longer exponential.) The higher modes ($p \ge 4$) seem to superpose well, indicating they have retained Rouse behavior. Let τ_p^* denote the time at which $\phi_p(t)$ decays to e^{-1}. KG's data clearly indicate that the ratio τ_p^*/τ_p increases rapidly as p decreases toward 1. The time window available to KG was not sufficiently long to obtain τ_1^* for $N = 100$. However, any reasonable extrapolation of the data for $\phi_1(t)$ to e^{-1} supports a large value for the ratio τ_1^*/τ_1 (see Figure 14c of ref 14). These two features of mode relaxations of longer chains are at variance with the reptation model of relaxation in a tube.[16,17] In this model, the original relaxation time of a Rouse mode p with $N/p > N_e$ is lengthened by a factor of N/N_e, but the relaxation function remains exponential.

$$\phi_p^{\text{rep}}(\tau) = \exp[-(t/\tau_p^{\text{rep}})] \tag{32}$$

$$\tau_p^{\text{rep}} = \frac{N\langle R^2\rangle}{p^2}\frac{\zeta}{\pi^2 k_B T}\frac{N}{N_e} \propto N^3/p^2 \tag{33}$$

Thus, the reptation model predicts that in a semilog plot the $\phi_p(t)$'s should be straight lines and they would collapse onto a single straight line if time for the p mode is scaled either by p^2 or by $(p/N)^2$. Neither of these predictions are borne our by KG's data of $N = 100$. KG has correctly pointed out that the generalized Rouse model (GRM) of Kovassalis and Noolandi[18] with the predictions of $\exp[-(t/\tau_p^{\text{GRM}})]$ for $\phi_p(t)$ and $\tau_p^{\text{GRM}} \propto N^3/p^4$ fair far worse than the reptation model when compared with their data. Nevertheless we cannot see how this state of affairs can justify the conclusion that their data strongly favor reptationlike concepts.

At first sight, the plot of ln $\phi_p(t)$ against scaled time, $t_p^2/\tau N^2$, for the $N = 200$ chains (Figure 16 of ref 14) appears to be close to collapsing onto a single curve when compared with the same plot (Figure 14c of ref 14) for the $N = 100$ chains. However, closer scrutiny of the manner in which the plot was made does not support this first impression. It is not fair to make a direct comparison between these two figures. Relative to that of Figure 14c for $N = 100$, the scale of the abscissa in Figure 16 for $N = 200$ is compressed by a factor of 4 due to N^{-2} in the p^2/N^2 scaling of t/τ and by another factor of 2 from the larger scaled time range (0–10 for $N = 200$ compared with 0–5 for $N = 100$) of the plot. These two factors amount to a combined total reduction by a factor of 8 in the distances of scaled time separation between different p modes. For $N = 100$ chains, the largest departures from linear exponential time dependence of $\phi(t)$ and from perfect superposition after scaling by p^2/N^2 are seen for the $p = 1$ mode. We certainly expect the same for the $N = 200$ chains. However, data of the $p = 1$ mode of $N = 200$ chains have decayed little within the available time window of $t/\tau < 15 \times 10^3$. Scaling time as $tp^2/\tau N^2$ for the $p = 1$ mode the entire data set $\phi_1(t)$ becomes invisible in the combined plot of $\phi_p(t)$'s for $p = 1$–6. If it were possible to acquire data at times much longer than $15 \times 10^3\tau$, then $\phi_1(t/\tau N^2)$ may exhibit an even larger departure from $\phi_p(tp^2/\tau N^2)$, obtained by scaling the time axis of the $p > 1$ modes, than the corresponding situation for $N = 100$ chains. It is important for us to point out that, although the data $\phi_p(t)$ for the higher modes, $p = 8$, 10, and 20, are available (Figure 13d of ref 14), they were not included by KG in their plots of $\phi_p(t)$ vs $tp^2/\tau N^2$ (Figure 16 of ref 14). Unlike the low p modes, these two higher p modes appear to have time dependences that are like exponential Rouse decay. When included in the Rouse scaling plot, they exhibit serious departures from superimposability with the lower p modes in the semilog plot of the ϕ_p's versus the scaled time $tp^2/\tau N^2$ (see Figure 1).

On the basis of the above discussion, we have no choice but to conclude that KG's data of the $N = 200$ chains are in substantial disagreement with the predictions of the reptation model, even more so than in the case of the $N = 100$ chains. On the other hand, as we shall immediately show, their data are remarkably consistent with the predictions of the coupling model.

Short chains with $N = 20$ and 50 studied by KG satisfy the conditions $N \leq N_e$ and $N < 2N_e$, respectively. From eq 1, the coupling parameters n_p either are all zero or at best assume some nonzero, but small, values. When n_p is zero or small, τ_p^* in eq 19 reduces back to the Rouse relaxation time τ_p, and the mode relaxation function given

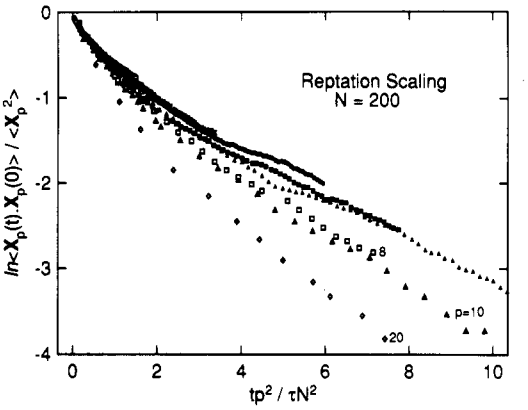

Figure 1. Relaxation plot for $\phi_p(t)$ from KG's data versus reptation or Rouse scaled time $tp^2/\tau N^2$ for the modes of $N = 200$. The symbols are the same as those used by KG in their Figure 13d.

by eq 22 becomes linear exponential function

$$\phi_p(t) = \exp[-(t/\tau_p)] \tag{34}$$

where

$$\tau_p = \frac{\zeta\langle R^2\rangle}{3\pi^2 k_B T}\frac{N}{p^2} \tag{35}$$

Longer chains with $N = 100$ and 200 satisfy the condition $N \gtrsim 2N_e$. Here N_e can be considered to be the characteristic length scale contained in the coupling model. The coupling parameters of the lower (smaller p) modes now assume nonzero values as indicated before by eq 5. For example, the $N = 100$ chains having $p_e \simeq 3$ imply at least that the coupling parameters n_p for $p = 1$ and 2 have values that are significantly above zero. From eq 22 a significant nonzero n_p gives rise to the stretched exponential relaxation function

$$\phi_p(t) = \exp[-(t/\tau_p^*)^{1-n_p}] \tag{36}$$

where the slower observed relaxation time, τ_p^*, can be calculated from the Rouse relaxation time τ_p by eq 19 provided ω_c is also known. If we rewrite eq 18 as

$$\tau_p^* = \{(1-n_p)^{1/(1-n_p)}[\omega_c\tau_p]^{n_p/(1-n_p)}\}\tau_p \equiv \Delta_p\tau_p \tag{37}$$

it becomes clear from the appearance of an extra factor multiplying τ_p on the right-hand side of eq 37 that the τ_p^*'s no longer scale as p^{-2} as the τ_p's do. The expected trend of the variation of n_p with p (see eq 5) and the sensitive dependence of Δ_p on p mean that the departure from the Rouse p^{-2} scaling depends on the mode number. We shall examine the p dependence of the extra factor Δ_p.

KG have given us an estimate of ω_c from their data of the mean-square displacement of the center of mass $g_{cm}(t)$. As discussed in a previous work,[11] the coupling model expects Rousean diffusion with

$$g_{cm}(t) = 6D_0 t \tag{38}$$

for $t < \omega_c^{-1}$ and slowed down diffusion with

$$g_{cm}(t) \sim t^{1-n_0} \tag{39}$$

for $\omega_c^{-1} < t \lesssim \tau_D^*$. For $N = 100$, KG reported that the onset of the slow down is at about 200τ. Hence we may identify ω_c^{-1} with this onset time and obtain

$$\omega_c = (200\tau)^{-1} \tag{40}$$

It is easy to verify from KG's data that normal modes of $N = 100$ and $N = 200$ chains with smaller p have their

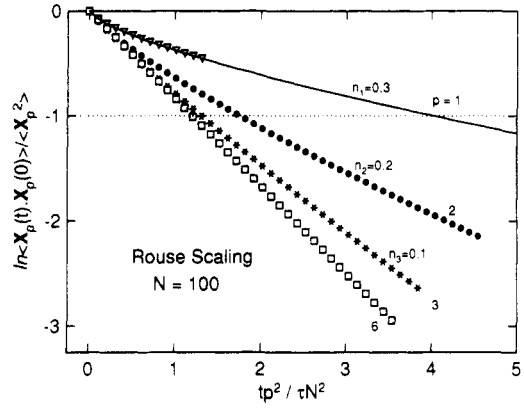

Figure 2. Semilogarithmic plot of the normal-mode autocorrelation function $\phi_p(t)$ against scaled time, $tp^2/\tau N^2$ for $N = 100$. The functions, $\phi_p(t)$ for $p = 1$–3 and 6 are calculated from the coupling scheme in the manner described in the text. The mode-dependent coupling parameters, n_p, are given here and in the text. Both the points and the solid lines represent the calculations of $\phi_p(t)$. The points are terminated at roughly the longest time reached by Kremer and Grest for that particular normal mode.

underlying (but not observed) Rouse relaxation times satisfying the condition

$$\omega_c \tau_p \gg 1 \tag{41}$$

Hence, Δ_p in eq 37 is larger than unity and makes τ_p^* longer than τ_p. On decreasing p, τ_p^*/τ_p increases rapidly because Δ_p increases rapidly due to larger $\omega_c\tau_p$ and, more importantly, to the increasing exponent $n_p/(1-n_p)$. The latter is a direct consequence of the property of the coupling parameters given by inequality eq 2; i.e., $n_p > n_{p'}$ if $p < p' < p_e$. The immediate consequences are as follows: (1) from eq 36, departure of $\phi_p(t)$ from linear exponential decay; (2) from eq 37, departure of τ_p^* (and hence the entire $\phi_p(t)$) from Rouse scaling with p as p^{-2}; and (3) these deviations become more serious with decreasing p. These features of the coupling scheme are actually found by KG and displayed clearly in their Figure 14c for $N = 100$. They are also present for the $N = 200$ chains but are obscured by the manner in which Figure 16 of ref 14 was presented as discussed above.

A direct comparison between the results of the coupling scheme and KG's normal-mode analysis data can be made. The $N = 100$ chains are still in the crossover region and are not fully entangled. From previous work based on[1] viscoelastic data, we found $n_1 = 0.41$ for fully entangled monodisperse linear polymer melts. This has been recently confirmed by dielectric measurements of the terminal relaxation.[19] For chains that are not fully entangled there is evidence[5,6,20] that n_1 is smaller. These estimates of n_p and inequality eq 5 suggest it is reasonable to assume for $N = 100$ chains that $n_1 \cong 0.30$, $n_2 = 0.20$, $n_3 = 0.10$, and $n_p = 0$ for $p \geq 4$. These choices for n_p, though arbitrary, but once made give results that semiquantitatively reproduce KG's data. The results obtained below should not be viewed as fits to KG's data although the essential features of the data are reproduced. With ω_c given by eq 40, and the estimate $\tau_6 \simeq 1.2(\tau N^2/6^2)$ from KG's $N = 100$ data, we can deduce from eq 35 τ_p for all other p's. Whence we can calculate τ_p^* from eq 37 and $\phi_p(t)$ from eq 36. The natural logarithm of the normal-mode relaxation functions for $p = 1$–3 and 6 is plotted against the Rouse scaled time $tp^2/\tau N^2$ in Figure 2. We have not taken into account the short-time Rouse decay according to $\exp[-(t/\tau_p)]$ for $\omega_c t < 1$. However, from the coupling model[21] this Rouse decay is negligible for $p = 1$–3 because $\omega_c\tau_p \gg 1$. The results obtained compare rather well with KG's data and reproduce all the essential features in Figure 14c of ref 14 semiquantitatively, i.e., deviations from exponential time dependence and Rouse p^2 scaling of the relaxation time, and increasing deviations with decreasing mode number. Had the actual data been available in tables rather than in figures, we would have fitted KG's data to eq 36 and determined τ_p^* and n_p for each mode. With n_p determined and ω_c known (eq 40), τ_p^* can be calculated from eq 37 and then compared quantitatively with the data.

In exactly the same manner we have calculated τ_p^* and $\phi_p(t)$ for the $N = 200$ chains with the choice of $n_1 = 0.40$, $n_2 = 0.30$, $n_3 = 0.20$, $n_4 = 0.10$, and $n_p = 0$ for $p \geq 6$. These choices of[1,4-6,21] values for the mode coupling parameters are again motivated by previous publications and past experience with real experimental data[1-6,19,21] guided by the expected trend (eq 5), the condition stated in eq 4, and the fact that $p_e \simeq 6$. We follow KG to scale t/τ by the Rouse factor p^2/N^2 and present the results in Figure 3 as a Rouse scaling plot. In this figure we include $\phi_p(t)$ for $p = 1$–3, 5, and 20. The calculated $\phi_p(t)$ for $p = 1$–3 and 5 plotted in the same manner as in their Figure 16 bear strong resemblances to KG's data. KG have not scaled the autocorrelation functions $\phi_p(t)$ for $p = 10$ and $p = 20$ to inlcude them in their Figure 16 although the data are available in their Figure 13d. Their $\phi_p(t)$ for $p = 20$ when approximated by an exponential function and plotted against the scaled time to $tp^2/\tau N^2$ corresponds very well to the solid curve labeled by $p = 20$ in Figure 3. In this figure, the solid curves represent the calculated ϕ_p's. The points are also the calculated values. They are terminated at approximately the longest $tp^2/\tau N^2$ carried out in KG's simulations, for that particular normal mode. Without the inclusion of $\phi_p(t)$ for $p = 20$ in the Rouse scaling plot, if we were unaware of the severe limit on $\phi_1(t)$ imposed by the time window and had we not been aware of the fact that the scale of the abscissa in Figure 3 here (Figure 16 in ref 14) is shrunk by a factor of 8 compared with that in Figure 2 here (Figure 14c in ref 14), we would follow KG to conclude either from our Figure 3 or from Figure 16 of Kremer and Grest that Rouse time scaling $t(p/N)^2$ seems to work reasonably well for $N = 200$, and reptation predictions give a good description of KG's data. The inclusion of $\phi_p(t)$ for $p = 20$ together with the plausible extrapolations of $\phi_1(t)$ and $\phi_2(t)$ to longer times (solid curves) in Figure 3 reveal that the $N = 200$ chains behave like the $N = 100$ chains. In both cases Rouse scaling fails and the small p mode relaxation functions are not linear exponentials but close to stretched exponentials. The failure of Rouse scaling is much more severe in the data for the $N = 200$ chains than in that for the $N = 100$ chains. This becomes evident if $\phi_p(t)$ were plotted against the scaling variable, tp^2/τ, instead of $tp^2/\tau N^2$, and the same scale for tp^2/τ was used in plotting $\phi_p(t)$ for $N = 100$ and $N = 200$. As pointed out earlier, KG's choice of the N-dependent scaled variable $tp^2/\tau N^2$ and their use of a smaller scale for it in plotting in the case of $N = 200$ has the effect of artificially reducing by a factor of 8 the degree of failure of Rouse scaling for $N = 200$ when comparing with the same for $N = 100$. In view of the present analysis, we are forced to disagree with KG in their conclusion that their data are in agreement with the original reptation predictions. Contrary to their claim, we find the data of normal modes provide strong evidence against the reptation hypothesis. On the other hand, essentially all the features of KG's data in Figures 2 and 3 can be reproduced by the coupling scheme. In particular, the coupling parameters n_p determined from KG's data have magnitudes consistent with the values that were determined in

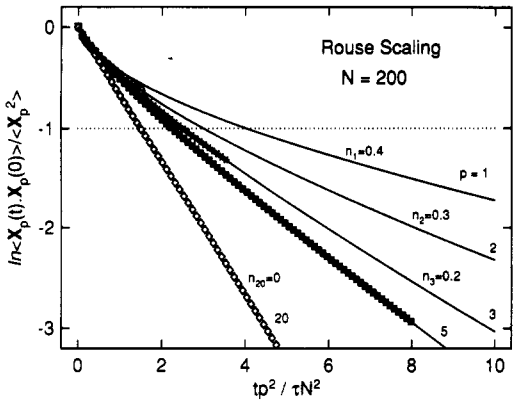

Figure 3. Semilogarithmic plot of the normal-mode autocorrelation function, $\phi_p(t)$, against scaled time, $tp^2/\tau N^2$, for $N = 200$ and $p = 1$–3, 5, and 20. The mode-dependent coupling parameters n_p are given here and in the text. Both the points and the solid lines represent the calculations of $\phi_p(t)$. The points are terminated at roughly the longest time reached by Kremer and Grest for that particular normal mode. We have plotted also the autocorrelation function for the $p = 20$ mode which was not included in Figure 16 of Kremer and Grest. With its inclusion, failure of Rouse scaling is evident. In comparing this figure for $N = 200$ with Figure 2 for $N = 100$ for the degree of failure of Rouse scaling, it is important to note that the scale of the abscissa here is reduced by a factor of about 8. A factor of 4 comes from the nonessential factor N^{-2} used in defining the scaled time, and another factor of 2 comes from the choice of a wider scaled time window, 0–10, for $N = 200$ as compared with 0–5 for $N = 100$, by Kremer and Grest.

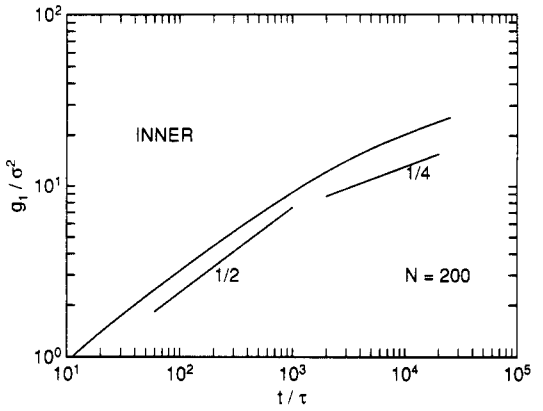

Figure 4. Mean-square displacement, $g_1^{\text{inner}}(t)$, vs t/τ averaged over the inner five monomers for $N = 200$ calculated from the coupling scheme with exactly the same parameters as used in Figure 3. The result shows that the t^α power law regime with $\alpha = 0.28 \pm 0.03$ obtained by KG is also consistent with the coupling model.

our previous publications[1-6,21] and are indicated here in eq 5. Thus, chain dynamics according to the coupling scheme are in good agreement with KG's data.

In all previous published works[1-6,11] as well as in the above discussions, the coupling scheme has been applied to the slowing down of Rouse modes of the *entire* chain only. Recently, Kremer and Grest[24] have looked at the Rouse modes of the *inner part* of the longest chain ($N = 200$). In the framework of the coupling scheme, motions of the monomers near the two ends of a chain involved in the low-p normal modes contribute significantly to coupling of the modes with that of other chains. In considering the Rouse mode of the inner part of the $N = 200$ chain, these important contributions to coupling from the monomers closer to the ends are removed. Moreover, by definition, the inner part of a chain necessarily has a shorter length than the entire chain. From previous discussions, we know that the Rouse modes of shorter chains in KG's simulation have smaller coupling parameters for the normal modes. Thus, we expect the Rouse mode of an inner part of the $N = 200$ chain is much less coupled than the $p = 1$ normal mode of the entire chain. Consequently the coupling parameter of any Rouse mode of an inner part of the $N = 200$ chain is significantly smaller than that of the corresponding normal mode of the entire chain. In the coupling model, small coupling parameters for the Rouse modes of the inner part of the 200 chain mean negligible modifications of the Rouse dynamics of these modes. In fact, the time dependences of relaxation of the inner part Rouse modes obtained by Kremer and Grest[24] from their simulation of a dense system look very similar to the autocorrelation functions calculated for the Rouse inner modes of a *single* chain.[25]

The Rouse modes of the inner part of the $N = 200$ chain thus have characteristics quite different from that of the entire chain. One should not blindly take over the results of the coupling scheme for the normal modes of the entire $N = 200$ chain as discussed above and assume they apply verbatim to the Rouse modes of the inner parts of the chain. This possible misuse of the coupling scheme to address the Rouse modes of the inner part of the chain may lead to contradiction which is not real.

B. Single-Bead Motion. The mean-square displacement of the ith bead along the chain $g_i(t)$ and the various average mean-square displacement per bead functions, $g_1(t)$ and $g_1^{\text{inner}}(t)$, have been given by eqs 24, 27 and 28, respectively, for the coupling scheme. We have evaluated $g_1^{\text{inner}}(t)$ for the $N = 100$ and 200 chains and compare the results with computer simulations. We follow KG and consider $g_1^{\text{inner}}(t)$ to be the average of $g_i(t)$ over the five innermost monomers. In evaluating $g_1^{\text{inner}}(t)$ from eqs 27 and 28, the set of coupling parameters n_p are the same as that used in the normal-mode analysis of the previous subsection for the $N = 200$ chains (Figure 3) as well as for the $N = 100$ chains (Figure 2). The τ_p*'s are calculated by eq 37 with ω_c given again by eq 40. Hence, all normal-mode relaxation parameters are the same as those that appear in Figures 2 and 3. With n_p and τ_p* known, $g_1^{\text{inner}}(t)$ can be calculated by eqs 24 and 28 which assume that the Rouse eigenvectors form a good basis set as was also done previously.[12] The results for $N = 200$ are shown as the solid curve in Figure 4. Deviation from the Rouse dependence $g_1^{\text{inner}}(t) \sim t^{1/2}$ is evident. The deviation is similar to KG's data. The deviation even starts at about the same t/τ. At longer times, the time dependence approaches a t^α power law with α about 0.29. Again, KG's data are very similar (see Figure 9 of ref 14) compared with our calculated $g_1^{\text{inner}}(t)$. We may conclude that their data for $g_1^{\text{inner}}(t)$ are reproduced essentially in a semiquantitative manner by the coupling model. We have shown the calculated values of $g_1^{\text{inner}}(t)$ up to $t = 10^4\tau$ because beyond that the center of mass motion, not included here, will start to make a significant contribution. It has already been shown, with the Rouse eigenvectors used as a basis set (see Figure 15 of ref 12), that the mean-square displacement of the outer monomers is larger than that of the inner monomers. The same is true here, but the results will not be repeated.

IV. Discussion and Conclusions

In this work, we have reformulated the coupling model for entangled polymer chains as a Fokker–Planck equation for Rouse chains generalized to include the time-dependent rate slowing down by entanglement couplings. The

essential physics proposed in the coupling scheme is recaptured. This new formulation enables us to continue to use the Rouse eigenvectors as a basis set but to modify the dynamics of the normal modes according to the coupling scheme. The relaxation of the lower p normal modes is slowed down if the chain length N exceeds a characteristic length N_e. Various relevant autocorrelation functions, $\phi_p(t)$, are obtained. The results from the coupling model have been compared with data of computer simulations, particularly in detail here with a molecular-dynamics simulation of Kremer and Grest (KG). A closer examination of the normal-mode analysis of KG's data reveals that they are in good agreement with the coupling model. Moreover, the essential features of the data, namely, a nonexponential relaxation function and the failure to superpose after Rouse scaling by $(p/N)^2$, contradict the original reptation predictions. We have also calculated $g_1^{\text{inner}}(t)$, the mean-square monomer displacement averaged over the inner monomers. The results are similar to the data of KG and exhibit an approximate t^α dependence in the intermediate time regime with $\alpha \simeq 0.29$, in agreement with KG's data and close to the value of $^1/_4$ predicted by the reptation model. Thus, as indicated previously, the existence of the approximately $t^{1/4}$ power law dependence can be reproduced by the coupling model and is not uniquely characteristic of reptation.[22-23]

In addition to $\phi_p(t)$ and $g_1^{\text{inner}}(t)$, good agreement between simulations[12-14] and the coupling model[2] was obtained on the center of mass mean-square displacement, $g_{cm}(t)$. This has been discussed in detail previously.[11] Recently a Monte Carlo simulation of polymer dynamics based on the bond fluctuation model[26] on a simple cubic lattice claimed to have obtained a feature in $g_{cm}(t)$ different from all previous simulations. This simulation found $g_{cm}(t) \sim t^{0.80}$ for $t \leq 3 \times 10^6$ Monte Carlo steps (MCS), $g_{cm}(t) \sim t^{0.50}$ for $3 \times 10^6 < t < 7 \times 10^6$ MCS, and $g_{cm}(t) \sim t^{0.90}$ for $t > 7 \times 10^6$ MCS. Emphasis was placed on the appearance in a time region of the dependence $g_{cm}(t) \sim t^{0.50}$ which had not been obtained before by any other simulations including that by Kremer and Grest. This is interesting also because such a time dependence for $g_{cm}(t)$ has been predicted by the reptation model. However, the time regime in which $g_{cm}(t) \sim t^{0.5}$ is only about a third of a decade, much shorter than that expected by the reptation model and required by consistency with the data of $g_1(t)$. If this feature of the data is to be taken seriously, then one must do the same for the $g_{cm}(t) \sim t^\delta$ dependence with $\delta \simeq 1.5$ in the time regime $6 \times 10^6 \lesssim t \lesssim 1 \times 10^7$ MCS that immediately follows. The anomalous kink defined by these two time dependences needs to be explained. It is not satisfactory to emphasize the $t^{0.5}$ dependence while ignoring the $t^{1.5}$ dependence. This time dependence of $g_{cm}(t)$, with an exponent approximately equal to 1.5, poses a problem for any known model including reptation because such a superlinear time dependence has not been predicted. It is not clear what exactly gives rise to this anomalous kink in the data. Before this is resolved, the $t^{0.5}$ dependence of $g_{cm}(t)$ observed as only a part of the kink in the simulation based on the bond fluctuation model may not be used as evidence for reptation.

In closing we point out two other approaches to the dynamics of entangled polymer liquids by Hess[27] and by Schweizer[28] that bear some relation to the coupling model. The essential physics in both theories is contained in a time-dependent friction coefficient which is similar to our time-dependent diffusion coefficient and drift term, eqs 11 and 12, in the Fokker–Planck formulation of the coupling scheme presented here. There are important differences however. Our time-dependent terms in eqs 11 and 12 come as products of the corresponding time-independent Rouse term and the slowing down factor $(\omega_c t)^{-n}$, while in the other approaches the time-dependent friction coefficient comes into the generalized Langevin equation as an additive term. In spite of the differences, we believe all these[27,28] are viable approaches to gain insight into the dynamics of polymer liquids.

Acknowledgment. This research was partially supported by a grant from the Polymers Program of the National Science Foundation, No. DMR 90-03872. (J.S.), and by ONR Contract N0001491WX 24019 (K.L.N.). We thank an anonymous reviewer for his insight and for sending us calculated autocorrelation functions of the Rouse modes for an inner part of a single chain. These calculations have helped us immensely in clarifying the difference in the effects many chain dynamics have on the normal mode of the entire chain and on the normal modes of an inner part of the same chain and confirm what we would have expected from the coupling model. K.L.N. thanks Prof. K. Binder for a preprint of the bond fluctuation model simulations.

Appendix

We give a general solution for the Fokker–Planck type equation with the coefficients $\beta(t)$ and $\gamma(t)$ which are functions of time

$$\partial_t P = \beta(t)\, \partial_\xi(\xi P) + \gamma(t)\, \partial_{\xi^2}{}^2 P \tag{A1}$$

Here we omit the subscript of mode, since the form of the equation is the same. To solve eq A1, we introduce a new variable[10]

$$\rho = \xi \exp\left(\int_0^t \beta(t')\, dt'\right) \tag{A2}$$

The equation becomes

$$\partial_t P = 3\beta(t)\, P + \gamma(t) \exp\left(2\int_0^t \beta(t')\, dt'\right) \partial_{\xi^2}{}^2 P \tag{A3}$$

We simplify eq A3 by a change of the variable

$$\chi = P \exp\left\{-3\int_0^t \beta(t')\, dt'\right\} \tag{A4}$$

to arrive at

$$\partial_t \chi = \gamma(t) \exp\left[2\int_0^t \beta(t')\, dt'\right] \partial_\rho{}^2 \chi \tag{A5}$$

The solution obtained with the initial condition

$$\rho = \rho(t_0) = \rho_0 \tag{A6}$$

is given by

$$\chi = [4\pi \int_0^t dt\, \gamma(t) \exp[2\int^t \beta(s)\, ds]^{-3/2} \times \exp\{-|\rho - \rho_0|^2/[4\int_0^t \gamma(\tau) \exp(2\int_0^t \beta(s)\, ds)\, d\tau]\} \tag{A7}$$

The probability P according eq A4 is given by

$$P(\xi,\xi_0;t) = \{\exp(\int_0^t \beta(\tau)\, d\tau)/4\pi \int_0^t \gamma(\tau) \times \exp[\int_0^\tau 2\beta(s)\, ds]\, d\tau\}^{3/2} \exp[-|\xi \exp(\int_0^t \beta(\tau)\, d\tau) - \xi_0|^2/4\int_0^t \gamma(\tau) \exp(\int_0^\tau 2\beta(s)\, ds)\, d\tau] \tag{A8}$$

Using relation eq 13 and noting that $\langle \xi_k{}^2 \rangle$ does not depend on time, the result in eq 18 in the text is obtained via eqs

11 and 7 as

$$P(\xi,\xi_0;t) = [2\pi\langle\xi^2\rangle(1-\exp(-\int_0^t 2\beta(s)\,ds))]^{-3/2}\exp[\xi(t) - \xi(0)\exp(-\int_0^t\beta(s)\,ds)]^2/\{2\langle\xi^2\rangle(1-\exp(-2\int_0^t\beta(s)\,ds))\} \quad \text{(A9)}$$

References and Notes

(1) Ngai, K. L.; Plazek, D. J. *J. Polym. Sci., Polym. Phys. Ed.* **1985**, *23*, 2159.
(2) McKenna, G. B.; Ngai, K. L.; Plazek, D. J. *Polymer* **1985**, *26*, 1651.
(3) Ngai, K. L.; Rajagopal, A. K.; Teitler, S. *J. Chem. Phys.* **1988**, *88*, 5086.
(4) Rendell, R. W.; Ngai, K. L.; McKenna, G. B. *Macromolecules* **1987**, *20*, 2250.
(5) Ngai, K. L.; Rendell, R. W. *Macromolecules* **1987**, *20*, 1066.
(6) Fytas, G.; Floudas, G.; Ngai, K. L. *Macromolecules* **1990**, *23*, 1104.
(7) Rouse, P. E. *J. Chem. Phys.* **1953**, *21*, 1273.
(8) Ferry, J. D. *Viscoelastic Properties of Polymers*; Wiley: New York, 1980.
(9) Ngai, K. L.; Rendell, R. W. *J. Non-Cryst. Solids* **1991**, *131–133*, 233. Rajagopal, A. K.; Ngai, K. L.; Teitler, S. *J. Phys. C* **1984**, *17*, 6611. Peng, S. L.; Ngai, K. L.; Tsang, K. Y., to be published.
(10) Chandrasekhar, S. *Rev. Mod. Phys.* **1943**, *15*, 1.
(11) Ngai, K. L.; Skolnick, J. *Macromolecules* **1991**, *24*, 1561.
(12) Kolinski, A.; Skolnick, J.; Yaris, R. *J. Chem. Phys.* **1987**, *84*, 1982; **1987**, *86*, 1567, 7165, 7174.
(13) Pakula, T.; Geyler, S. *Macromolecules* **1987**, *20*, 2909; **1988**, *21*, 1665.
(14) Kremer, K.; Grest, G. S. *J. Chem. Phys.* **1980**, *92*, 5057.
(15) Skolnick, J.; Yaris, R. *J. Chem. Phys.* **1988**, *88*, 1418 and references therein.
(16) de Gennes, P.-G. *J. Chem. Phys.* **1971**, *55*, 572; **1980**, *72*, 4756.
(17) Doi, M.; Edwards, S. F. *J. Chem. Soc., Faraday Trans. 2* **1978**, *74*, 1789; **1978**, *74*, 1802; **1978**, *74*, 1818; **1978**, *75*, 38.
(18) Kavassalis, T. A.; Noolandi, J. *Phys. Rev. Lett.* **1987**, *59*, 2674; *Macromolecules* **1989**, *22*, 2720.
(19) Boesse, D.; Kremer, F.; Fetters, L. J. *Macromolecules* **1990**, *23*, 829.
(20) Ngai, K. L.; Plazek, D. J., unpublished results.
(21) Ngai, K. L.; Rendell, R. W.; Rajagopal, A. K.; Teitler, S. *Ann. N.Y. Acad. Sci.* **1986**, *484*, 150.
(22) Melek, M.; Kolinski, A.; Skolnick, J. *J. Chem. Phys.* **1990**, *93*, 4440.
(23) Skolnick, J.; Kolinski, A. *Adv. Chem. Phys.* **1990**, *78*, 223.
(24) Kremer, K., private communication.
(25) The method and the results of calculating Rouse inner modes of a single chain were supplied by an anonymous reviewer of this paper.
(26) Paul, W.; Binder, K.; Heermann, D. W.; Kremer, K., preprint.
(27) Hess, W. *Macromolecules* **1986**, *19*, 1395; **1987**, *20*, 2589; **1988**, *21*, 2620.
(28) Schweizer, K. S. *J. Chem. Phys.* **1989**, *91*, 5802; **1989**, *91*, 5822; *J. Non-Cryst. Solids* **1991**, *131–133*, 643.